

Analyzing Cross-Phase Effects of Reactive Power Intervention on Distribution Voltage Control

Dhaval Dalal, *Senior Member, IEEE*, Anamitra Pal, *Senior Member, IEEE*, and Raja Ayyanar, *Fellow, IEEE*
School of Electrical, Computer and Energy Engineering
Arizona State University, Tempe, AZ, USA
ddalal2@asu.edu, anamitra.pal@asu.edu, rayyanar@asu.edu

Abstract—Increasing photovoltaic (PV) penetration in the distribution system can often lead to voltage violations. Mitigation of these violations requires reactive power intervention from PV inverters. However, the unbalanced nature of the distribution system leads to mixed effects on the voltages of nearby nodes for each inverter injecting or absorbing reactive power. In particular, reactive power absorption to reduce over-voltage in one phase can exacerbate over-voltage in a different phase. In this paper, the factors impacting the incremental and decremental voltage effects of reactive power intervention are analyzed in detail. The result of these effects on the distribution system performance is presented to highlight their significance and the need to factor them in for any coordinated voltage control algorithm.

Index Terms—Cross-phase effects, Photovoltaic penetration, Reactive power intervention, Voltage control

I. INTRODUCTION

The road to net zero emissions (NZE) has milestones for achieving significantly high level of photovoltaic (PV) penetration in the distribution systems [1]. However, due to limited planning control and operational visibility from the utility side, the proliferation of PVs can lead to potential voltage violations which negatively impact the distribution system quality and reliability [2]. The contributors to voltage violations include a combination of factors such as power flow reversal, low X/R ratio, inappropriate settings of step voltage regulators (SVRs) and capacitor banks (CBs), and sudden drastic changes in PV generation and load profiles [3].

Two major avenues for addressing the voltage violations are: (a) on-load-tap-changer (OLTC)/SVR/CB control, or (b) reactive power (Q) intervention (e.g., injection or absorption) from PV inverters. A combination of the two provides a third option. OLTC/SVR/CB control has severe maintenance cost penalty if implemented to address the diurnal variations in PV generation. Hence, the focus of current research is on inverter Q control. Localized voltage control techniques such as inverter volt-VAr (VV) control require no coordination, but have limited effectiveness when the PV penetration is high [4]. Communication-based methodologies, in which the inverters are actively monitored and commanded in a coordinated fashion using information not locally available to each inverter, are more effective for PV-rich systems [5], [6]. Since coordinated control on large distribution systems

have significant communication and computation overhead, a number of recent works have proposed decentralized voltage regulation by partitioning the distribution networks into zones [7], [8]. However, any partitioning of the system results in certain parametric effects being ignored, because they cannot transcend the partition boundaries. Specifically, the unbalanced nature of distribution systems create significant cross-phase voltage effects, often leading to new voltage violations when Q intervention is used in a single-phase PV inverter. Since many of the zoning approaches rely on phase-based partitions (e.g., [7]–[9]), the cross-phase effects are disregarded, resulting in sub-optimal outcomes.

In this paper, a methodical approach is developed to characterize the cross-phase voltage effects caused by Q intervention, including their causes, sensitivities, and end-effects on system performance. The value of considering these effects is demonstrated by testing on a renewable-rich complex feeder¹ with and without these effects factored in.

The major contributions of this paper are as follows:

- Identification of cross-phase voltage effects as a major impediment in achieving desired voltage regulation in distribution networks with high PV penetration
- Sensitivity analyses to identify and quantify the factors impacting cross-phase voltage effects
- Proposing and validating a novel methodology to integrate cross-phase voltage effects into a voltage regulation algorithm to achieve higher hosting capacity (HC)

II. CHARACTERISTICS OF UNBALANCED DISTRIBUTION SYSTEMS

Distribution systems are significantly different from transmission systems in terms of power flow balance between phases, line impedances, and/or types of distributed energy resources (DERs). The role of these factors in maintaining reliable system operation is well understood for traditional load-dominant distribution systems or systems with low levels of DER penetration [10]. However, there is a need to investigate the behavior of distribution systems with a high percentage of DERs that are participating in voltage regulation by injecting or absorbing significant levels of Q. Following characteristics of distribution systems merit special attention:

¹This work was supported in part by the US Department of Energy under grant DE-EE0009355.

¹A complex feeder is one that has both primary and secondary circuits, unbalanced multi-phase lines/loads, and OLTCs/SVRs/capacitors.

- 1) **Low X/R ratios:** Smaller conductor sizes in the distribution system lead to much larger increases in the per unit resistance values ($\propto \frac{1}{d^2}$) compared to the increases in (self and mutual) inductances ($\propto \log \frac{1}{d}$). For instance, X/R ratios in many distribution systems are in between 2 and 4 as compared to >10 for transmission systems.
- 2) **Diversity of line configurations:** Distribution systems consist of single-phase, two-phase, and untransposed three-phase lines serving unbalanced loads. Therefore, a positive sequence analysis approach is not valid. As stated in [10], “it is necessary to retain the identity of the self- and mutual impedance terms of the conductors in addition to taking into account the ground return path for the unbalanced currents”.
- 3) **DER types:** The addition of behind-the-meter DERs (typically, PVs) is not controlled by the utilities. They are likely to add to the phase imbalance caused by the loads, while also adding high degrees of uncertainty and variability. Particularly, the PV inverters have varying capability to inject or absorb Q.

In summary, when voltage mitigation is done in PV-rich systems by providing Q absorption/injection, the imbalance and low X/R ratios play a major role in determining the outcome of the Q intervention [11].

III. SIMPLE DISTRIBUTION SYSTEM ILLUSTRATION

To fully understand the effects of Q intervention in distribution networks, it is useful to first construct a simple 4-wire, 2-bus system as shown in Fig. 1. Note that this system is a reduced version of the 4-bus test case available in OpenDSS, with the transformer removed and the feeder-head line-to-line voltage changed to 4.16 kV. All other configuration details including wire data, line geometry, and load were retained from the original case. The system has a balanced 3-phase load (5400 kW, 0.9 power factor (PF)), representing the base case ($i = 0$). A primitive impedance matrix, $Z_{prim} \in \mathbb{R}^{4 \times 4}$, consisting of Z_{mut} and Z_{earth} components was constructed from the available data using modified Carson’s equations. With the given parameters, the X/R ratio is about 3:1. The power flow equations are given by:

$$\mathbf{S}_i = \mathbf{P}_i + j\mathbf{Q}_i \quad (1)$$

$$\mathbf{I}_{L_i} = \left(\frac{\mathbf{S}_i}{\mathbf{V}_{N4_i}} \right)^* \quad (2)$$

$$\mathbf{V}_{N4_i} = \mathbf{V}_S - \mathbf{I}_{L_i} \times Z_{prim} \quad (3)$$

where, \mathbf{S}_i , \mathbf{P}_i , and \mathbf{Q}_i are the load apparent, real and reactive power vectors, \mathbf{I}_{L_i} is the complex vector representing the line current, * in the superscript denotes the conjugate operation, \mathbf{V}_S is the base voltage vector (a constant), and \mathbf{V}_{N4_i} is the voltage vector at the load node. It was observed that despite a balanced load, the \mathbf{V}_{N4_0} values exhibited imbalance, which is attributable to the mutual impedance mismatches related to wire location differences. The results obtained by solving (1)-(3) numerically were found to be consistent with those

obtained from the OpenDSS solution of this system. The phase voltage magnitudes are shown in the first row of Table I.

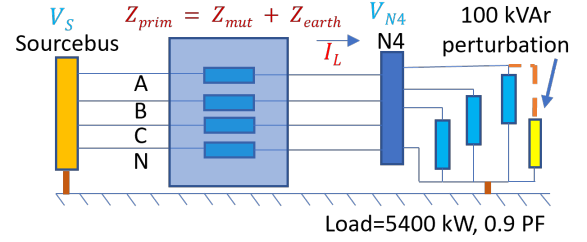


Fig. 1: Simple 4-wire, 2-bus system

Next, a perturbation of 100 kVar ($Q_{1_a} = Q_{0_a} + 100$ kVar) is applied to phase A to test the effects of PV inverter Q absorption ($i = 1$). Solutions to (1)-(3) were again found to be consistent with the OpenDSS results. The phase voltage magnitudes are provided in the second row of Table I. The voltage difference between the two cases is shown in the third row of the table. Since the objective of Q absorption is to reduce the voltage, the results for phase A are consistent with that objective. However, it is observed that both phase B and phase C have voltage differences of opposite polarity.

TABLE I: N4 phase voltages (in Volts)

Case	Phase A	Phase B	Phase C
Base ($i = 0$)	2103	2206	2150
+100 kVar ($i = 1$)	2068	2217	2160
Difference	-35.3	11.6	10.0
Difference due to Z_{earth}	19.2 $\angle 180^\circ$	19.2 $\angle 180^\circ$	19.2 $\angle 180^\circ$
Difference due to Z_{mut}	16.4 $\angle 165^\circ$	2.1 $\angle -57^\circ$	3.4 $\angle 57^\circ$

Before providing contextual analysis of these results, it is instructive to find the contributions to the voltage differences from Z_{earth} ($\Delta \mathbf{V}_{N4_e}$) and Z_{mut} ($\Delta \mathbf{V}_{N4_m}$), respectively. Note that this breakdown is not available from the OpenDSS power flow results, but can be obtained by solving the following equations that decompose the contributions. The dominant component of $\Delta \mathbf{I}_L$ is the imaginary component of phase A. It leads to the computed values of $\Delta \mathbf{V}_{N4_e}$ and $\Delta \mathbf{V}_{N4_m}$ from (5) and (6), respectively, which are shown in the last two rows of Table I.

$$\Delta \mathbf{I}_L = \mathbf{I}_{L_1} - \mathbf{I}_{L_0} \quad (4)$$

$$\Delta \mathbf{V}_{N4_e} = \Delta \mathbf{I}_L \times Z_{earth} \quad (5)$$

$$\Delta \mathbf{V}_{N4_m} = \Delta \mathbf{I}_L \times Z_{mut} \quad (6)$$

The results in Table I provide significant insights into the incremental and decremental effects of changes in reactive power (ΔQ). The positive voltage deviations in phases B and C as a result of Q absorption in phase A show unintended consequences of a corrective action (i.e., voltage mitigation for phase A) that must be recognized. Additionally, the decomposition of the contributions from Z_{mut} and Z_{earth} show that the corrective effect for phase A has nearly equal and significant contributions from both factors, while the phase

B and phase C effects are dominated by the Z_{earth} factor (compare the entries in the last two rows of Table I for phases B and C). To understand why the earth current has such a large opposite-polarity effect on the other phases, we look at the phasor diagrams of the voltages in Fig. 2. Individual phasors are color coded and their values are shown next to the diagrams for clarity.

For phase A, the contributions from Z_{mut} and Z_{earth} have similar phase and magnitudes, and the combination of the two results in phase A voltage reduction (which is expected). Since the earth current is the same, the ΔV_{N4_e} is identical for all three phases, as depicted by the vectors in black color and values in the phasor diagrams. Moreover, since the perturbation was made in phase A, the effects of Z_{mut} on phases B and C voltages are minimal as shown by the red-

colored vectors and values. As a result, the composite effect of ΔV_{N4} for phases B and C is dominated by the ΔV_{N4_e} component, which is 19.2 V at -180° . As seen in Figs. 2b and 2c, the phasor addition of ΔV_{N4} and V_{N4_0} for phases B and C result in higher magnitudes of V_{N4_1} with a very small change in angle.

While these results allow a good analytical basis for understanding the cross-phase effects and their causes, they need to be put into proper context. Firstly, the reported voltage deviations are fairly small in p.u. terms (-0.015 p.u. for phase A, and about 0.005 p.u. for phases B and C). Secondly, a real distribution system rarely has the 4-wire line configuration shown in Fig. 1 with a single-phase PV on one of the lines. Hence, the question to address is whether actual distribution systems need to contend with both incremental and decremental effects when using Q intervention from DERs as a voltage control technique. This is analyzed in the next section.

IV. EVALUATION ON A COMPLEX DISTRIBUTION SYSTEM

For this purpose, we evaluate the J1 Feeder [12], which represents a distribution system in the U.S. Northeast, with open-source data and models provided by EPRI. Key attributes of the feeder are summarized in Table II. In addition, J1 has a diverse mix of underground and overhead lines with different impedance characteristics and single-phase loads/transformers ranging from 0.3 kW/5 kVA to 20 kW/75 kVA. With this level of complexity, the phasor-based approach used in the previous section may not yield sufficient insights. Instead, the results from OpenDSS are used to perform the analysis. Since there is no time series data available for the J1 feeder, data from Pecan Street [13] were applied to the loads and PVs in the J1 feeder to perform the analysis across different time instants.

TABLE II: Attributes of EPRI J1 feeder

Parameter	Value	Comments
Primary Voltage	12.47 kV	Substation transformer at 69 kV
Secondary Voltage	240 V	
Total Customers	1384	363/375/643/3 (Phase A/B/C/3-ph)
Total Nodes	4245	2037 Primary/2208 Secondary
Total Load	10.95 MW	Includes 5 MW aggregated load
Transformers	819	218/225/372/4 (Phase A/B/C/3-ph)
SVRs	9	3/3/2/1 (Phase A/B/C/Substation)
Capacitors	3900 kVAR	5 Capacitors
Existing PV	1813.6 kW	1.71 MW commercial, 103.6 kW residential

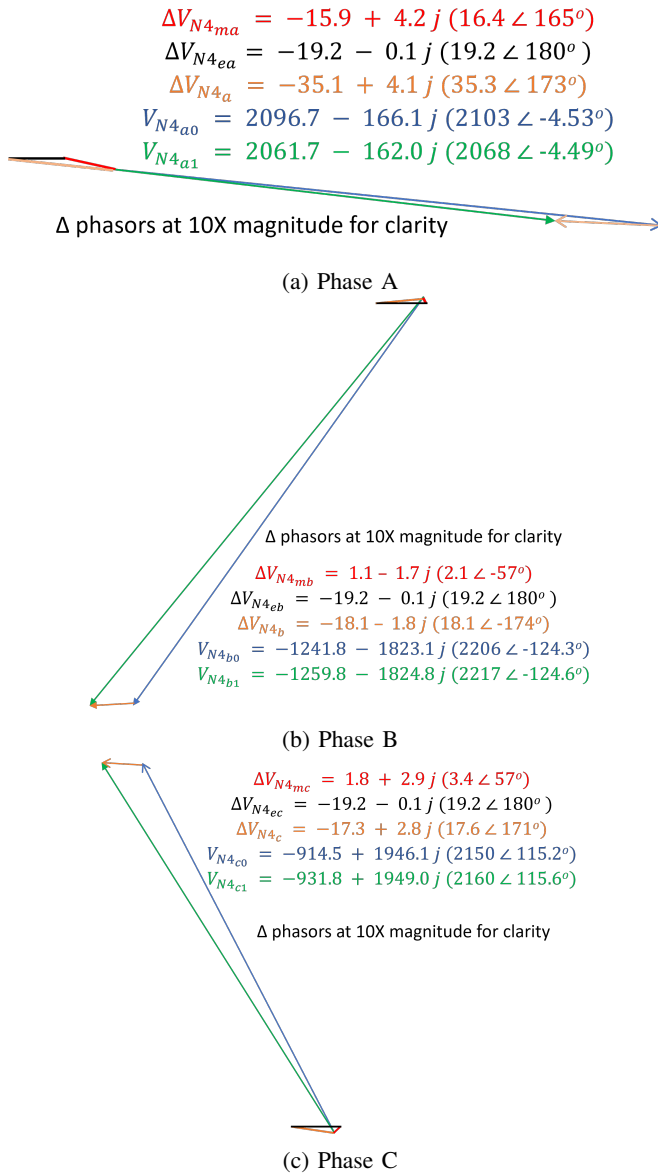


Fig. 2: Phasor diagrams showing effects of Q perturbation

A. Effect of Reactive Power (Q) Intervention from PV Nodes

To increase the J1 feeder HC without incurring voltage violations, an extreme use case (11 AM, August) was selected. For this use case, a voltage-reactive power sensitivity matrix (VQ-SM) was constructed, with its elements given by (7), where ΔQ_j is the reactive power perturbation applied to PV inverter j , and v_i^0 and $v_{i,j}^Q$ are the voltages at node i prior to the perturbation and after the perturbation, respectively.

$$sm_{i,j} = \frac{v_{i,j}^Q - v_i^0}{\Delta Q_j} \quad (7)$$

Since the VQ-SM is large (rows corresponding to number of PVs and columns corresponding to number of nodes in the system) we can look at one column which depicts the effect on a single system node from all the PVs where ΔQ can be applied. It was observed that the secondary node of a single-phase SVR in phase B, B19007reg.2, exhibited highest voltage on a consistent basis under moderate-to-high PV penetration. This SVR is located downstream from the feeder-head and has a step-up ratio to restore the voltage levels under high load conditions. At 11 AM, when PV generation is high with moderate load conditions, the voltage on the primary side of the SVR goes up (but does not have violations). However, due to the step-up ratio, the secondary node and other nodes close to the SVR (including some customer sites) experience voltage violations. The method to address these violations is to identify PV nodes that have the highest impact on this SVR secondary node and activate them for Q intervention. Fig. 3 depicts the sensitivity of all the PV nodes in the system to the selected node (B19007reg.2).

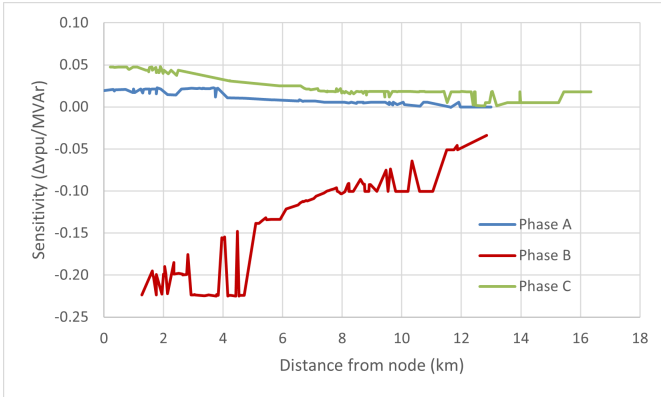


Fig. 3: Sensitivity of a single SVR node to all PVs

The following observations are made from Fig. 3:

- Sensitivity values for phase B absorption are negative as the node under consideration is a phase B node. Both phase A and phase C sensitivities are positive - a result consistent with the explanation in Section III.
- The sensitivity magnitudes generally decrease as the distance from the node increases. However, there are clear exceptions indicated by the choppiness of the plots. These can be attributed to the fact that the physical distances do not always equate to the electrical distances (impedances). Additional factors such as the presence of CBs and SVRs, and location relative to the substation (upstream or downstream) also contribute to these incongruous results.
- If only the Q interventions of phase B are considered to address the voltage violations, it may not be sufficient. This is because many of the nearby PVs in phases A and C may be activated to address voltage violations in the nodes located on those phases, and they could trigger decremental effects on the selected SVR node. Hence,

one must consider all phase effects together to achieve the desired results.

The inferences drawn from these observations are used to implement an empirical prioritized voltage control strategy that is explained in the next sub-section.

B. Prioritized Q Intervention for Effective Voltage Control

An empirical Algorithm 1 is now devised to add PVs into a distribution system for increased HC while accounting for the cross-phase effects explained previously. The main purpose of this algorithm is to provide a relatable illustration of the cross-phase effects and the means to overcome them.

Algorithm 1 PV addition/Voltage control algorithm

- 1: Load network details into a distribution system solver
 - 2: Add n PV system, where $n = 1$
 - 3: Apply appropriate PV and load profiles
 - 4: Select evaluation condition (time instance)
 - 5: Run power flow with unity PF (UPF) and identify locations and values of voltage violations by phase
 - 6: Identify PVs with highest sensitivity to the UPF violation nodes and incrementally add ΔQ on them till zero violations are achieved in power flows
 - 7: Repeat Steps 3 to 6 with $n = n + 1$ PVs
-

The results of running Algorithm 1 on EPRI J1 feeder are depicted in Fig. 4. These results clearly identify the decremental effects of uncoordinated Q intervention. As shown in the first two rows, for 90 PV additions, all violations are in phase B (68 of them), and they were addressed (Step 6) by activating Q intervention in a prioritized list of 15 PVs in phase B, guided by the VQ-SM. When 10 more PVs were added (Step 7a), there were more phase B violations (121 of them), but no phase A or phase C violations under UPF. However, when the Q intervention from Step 6 was activated (Step 7b), there were two new violations in phase A. The dominant contributor to the new violations in phase A was the decremental effect from Q intervention on the 15 phase B PVs. This was further confirmed by reducing the Q intervention in phase B, which removed the phase A violation, but reintroduced the phase B violations. The final solution, as shown in the last row (Step 7c), was to add Q intervention at one phase A PV.

V. IMPACT ON VOLTAGE CONTROL STRATEGIES

The simple example in Section IV-B clearly showed the decremental effect of cross-phase sensitivity. Looking at the larger picture, it also points to the challenges in achieving effective coordinated voltage control with Q intervention in real-world, large, complex distribution systems. For example, with any partition that is phase-based or distance-based, there will be a significant loss of accuracy that can lead to sub-optimal results from a voltage control perspective.

In order to demonstrate this impact, a large number (460) of residential PVs were added in a random fashion to the EPRI

Step	Action	Result
2-5	+90 PVs, run UPF	68 Violations (Phase B)
6	Q for 15 PVs (Phase B)	0 Violations
7a	+10 PVs, run UPF	121 Violations (Phase B)
7b	Same Q as Step 6	2 Violations (Phase A)
7c	Q for +1 PV (Phase A)	0 Violations

Fig. 4: Cross-phase sensitivity effects using Algorithm 1

J1 feeder, taking the total PV capacity to 6.4 MW. With the inverters set at UPF (i.e., without any Q intervention), there were many voltage violations for different hours of the day with the maximum voltage exceeding 1.1 p.u. during some hours as shown in the left part of Fig. 5.

Next, the network is partitioned into three zones, one for each phase. For each phase, a VQ-SM is created using only the PVs and nodes in that phase, and three optimization algorithms are run independently of each other for the three phases. The goal of each of the optimization algorithms was to find the minimum Q intervention in a given phase to minimize the voltage violations of that phase. The results from the three algorithms are combined and applied to the distribution system solver (OpenDSS) to check for voltage violations. The results in the middle part of Fig. 5 clearly depict the relative ineffectiveness of the phase-based partitioning. By omitting the cross-phase sensitivity from the optimization formulation, the optimizer is misled into providing Q intervention solutions that may work for one phase, but not for the other phases.

Finally, an optimization-based iterative voltage control algorithm was developed to mitigate the violations, while also accounting for the cross-phase sensitivity effects. This algorithm relied on availability of system-wide voltage information and iterative refinement of the VQ-SM for its effectiveness. More details about this algorithm can be found in [14]. As shown in the right part of Fig. 5, this algorithm is successful in removing voltage violations at all hours, which is impressive considering the extent of violations in the UPF case in terms of numbers (3000+) and voltage magnitudes (1.1045 p.u.).

VI. CONCLUSION

This paper presented a robust argument for considering the cross-phase effects of Q intervention in distribution systems to achieve better voltage control and higher levels of HC. The underlying reasons for the cross-phase sensitivity were identified first. Then, a simple network model was created and phasor diagrams were employed to analytically depict how the cross-phase effects manifest in the system.

Next, successive illustrations on a complex real-world distribution feeder underlined how the cross-phase effects negatively impact voltage control algorithms if they are not fully

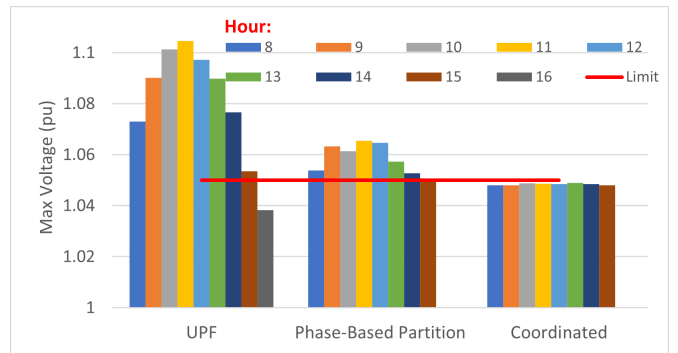


Fig. 5: Cross-phase sensitivity effects with high PV penetration

considered within the control strategy. Finally, a demonstration of how the incorporation of these effects in the control algorithms lead to significantly better results was provided.

REFERENCES

- [1] SolarPower Europe, "Global market outlook for solar power 2023-2027." [Online]. Available: <https://www.solarpowereurope.org/insights/outlooks/global-market-outlook-for-solar-power-2023-2027/detail#global-solar-market-update-2000-2022>
- [2] T. S. Ustun, J. Hashimoto, and K. Otani, "Impact of smart inverters on feeder hosting capacity of distribution networks," *IEEE Access*, vol. 7, pp. 163 526–163 536, 2019.
- [3] E. Demirok, P. C. González, K. H. B. Frederiksen, D. Sera, P. Rodriguez, and R. Teodorescu, "Local reactive power control methods for overvoltage prevention of distributed solar inverters in low-voltage grids," *IEEE Journal of Photovoltaics*, vol. 1, no. 2, pp. 174–182, 2011.
- [4] F. Ding and B. Mather, "On distributed PV hosting capacity estimation, sensitivity study, and improvement," *IEEE Transactions on Sustainable Energy*, vol. 8, no. 3, pp. 1010–1020, 2017.
- [5] P. Lusi, L. L. H. Andrew, A. Liebman, and G. Tack, "The added value of coordinating inverter control," *IEEE Transactions on Smart Grid*, vol. 12, no. 2, pp. 1238–1248, 2021.
- [6] Y. Yao, F. Ding, K. Horowitz, and A. Jain, "Coordinated inverter control to increase dynamic PV hosting capacity: A real-time optimal power flow approach," *IEEE Systems Journal*, vol. 16, no. 2, pp. 1933–1944, 2022.
- [7] P. Li, C. Zhang, Z. Wu, Y. Xu, M. Hu, and Z. Dong, "Distributed adaptive robust voltage/var control with network partition in active distribution networks," *IEEE Transactions on Smart Grid*, vol. 11, no. 3, pp. 2245–2256, 2020.
- [8] B. Zhao, Z. Xu, C. Xu, C. Wang, and F. Lin, "Network partition-based zonal voltage control for distribution networks with distributed PV systems," *IEEE Transactions on Smart Grid*, vol. 9, no. 5, pp. 4087–4098, 2018.
- [9] A. Alrushoud, C. McEntee, and N. Lu, "A zonal Volt/VAr control mechanism for high PV penetration distribution systems," in *2021 IEEE Power and Energy Society General Meeting (PESGM)*, 2021, pp. 1–5.
- [10] W. Kersting, *Distribution System Modeling and Analysis*. Taylor & Francis, CRC Press, 2017. [Online]. Available: <https://books.google.com/books?id=TnJIvWEACAAJ>
- [11] T. Niknam, "A new HBMO algorithm for multiobjective daily Volt/VAr control in distribution systems considering distributed generators," *Applied energy*, vol. 88, no. 3, pp. 778–788, 2011.
- [12] Electric Power Research Institute, "EPRI Test Circuits J1 Feeder OpenDSS Code." [Online]. Available: https://sourceforge.net/p/electricdss/code/HEAD/tree/trunk/Distrib/EPRI/TestCircuits/epr/_dvp/J1/
- [13] Pecan Street Research Institute, "The Dataport Database." [Online]. Available: <https://pecanstreet.org/dataport/>
- [14] D. Dalal, M. Sondharangalla, R. Ayyanar, and A. Pal, "Improving Photovoltaic Hosting Capacity of Distribution Networks with Coordinated Inverter Control – A Case Study of the EPRI J1 Feeder," 2023. [Online]. Available: <https://arxiv.org/abs/2311.02793>